FUNCTIONAL CONNECTOME CONTRACTIONS IN TEMPORAL LOBE EPILEPSY

Sara Larivière[1], Yifei Weng[2], Reinder Vos de Wael[1], Birgit Frauscher[3], Zhengge Wang[4], Andrea Bernasconi[5], Neda Bernasconi[5], Dewi V. Schrader[6], Zhiqiang Zhang[*2], Boris C. Bernhardt[*1]

[1]*Multimodal Imaging and Connectome Analysis Laboratory, McConnell Brain Imaging Centre, Montreal Neurological Institute and Hospital, McGill University, Montreal, QC, Canada;* [2]*Department of Medical Imaging, Jinling Hospital, Nanjing University School of Medicine, Nanjing, China;* [3]*Montreal Neurological Institute and Hospital, McGill University, Montreal, QC, Canada;* [4]*Department of Radiology, Nanjing Drum Tower Hospital, The Affiliated Hospital of Nanjing University Medical School, Nanjing, China;* [5]*NeuroImaging of Epilepsy Laboratory, McConnell Brain Imaging Centre, Montreal Neurological Institute and Hospital, McGill University, Montreal, QC, Canada;* [6]*BC Children's Hospital, Department of Pediatrics, University of British Columbia, Vancouver, BC, Canada*

[*] *authors contributed equally*

CORRESPONDENCE TO:
Boris C. Bernhardt, PhD
Montreal Neurological Institute (NW-256)
3801 University Street
Montreal, Quebec, Canada H3A 2B4
Telephone: (514) 398-3579
E-mail: boris.bernhardt@mcgill.ca

Sara Larivière, PhD Candidate
E-mail: sara.lariviere@mail.mcgill.ca

ABSTRACT

OBJECTIVE. Temporal lobe epilepsy (TLE) is classically associated with hippocampal pathology, and increasingly with structural changes beyond the mesiotemporal lobe. Functional anomalies, their link to cortical morphology and microstructure, and their utility in surgical prognosis, however, remain less well understood.

METHODS. We studied 30 drug-resistant TLE patients and 57 healthy controls using multimodal 3T MRI. All patients had histologically-verified hippocampal sclerosis and underwent post-operative imaging to establish the extent of surgical resection. Our analysis leveraged a novel resting-state fMRI framework that parameterizes functional connectivity distance, consolidating functional and geometric properties of macroscale brain networks. Functional findings were integrated with morphological and microstructural metrics, and associations to post-surgical seizure outcome were examined using machine learning techniques.

RESULTS. Compared to controls, TLE showed connectivity distance reductions in temporo-insular and dorsomedial prefrontal networks, with the former being more marked ipsilateral to the focus. Findings were driven by contractions in long-distance connections together with an excess in short-range connections, suggesting topological segregation of functional networks. Parallel structural profiling indicated that functional connectivity distance reductions in TLE were independent of atrophy but mediated by microstructural changes in the underlying white matter. Patients with persistent seizures showed anomalies a distinct network signature which predicted seizure outcome with 75±4% accuracy (using 5-fold cross-validation).

CONCLUSIONS. Our findings suggest connectivity distance contractions as a pathoconnectomic substrate of TLE. Functional topological isolation may represent a microstructurally mediated network mechanism that tilts the balance towards epileptogenesis in affected networks.

KEY WORDS: Epilepsy, connectome, networks, neuroimaging, outcome

INTRODUCTION

Temporal lobe epilepsy (TLE) is a recognized surgically-amenable disorder and ranks among the most prevalent drug-resistant adult epilepsies. While traditionally conceptualized as a prototypical "focal" epilepsy with a mesiotemporal epicenter, mounting histopathological and neuroimaging evidence has shown structural and functional compromise affecting widely distributed brain networks, supporting the notion of TLE as a system disorder affecting large-scale networks.[1] In effect, adequately capturing its connectopathy may advance our understanding of brain mechanisms giving rise to temporal lobe seizures, improve diagnostic procedures of individual patients, and guide surgical prognostics.

Paralleling prior studies mapping whole-brain structural alterations in TLE via volumetric[2-4] and diffusion MRI techniques,[5, 6] recent years have witnessed a surge in resting-state functional MRI (rs-fMRI) analyses.[7, 8] Given its versatility to probe multiple functional systems within a single acquisition, rs-fMRI represents a candidate technique to identify network mechanisms and biomarkers of brain disorders. Initial rs-fMRI investigations have targeted connectivity alterations in TLE compared to controls in specific networks, showing mainly decreased connectivity when focussing on mesiotemporal circuits,[9 10] on the interplay of mesial and lateral temporal regions,[11] or when studying connectivity between temporal seeds and macroscale networks, particularly the so-called "default-mode" network.[12, 13] One such study revealed that degrees of hippocampal structural damage correlated with reductions in hippocampal functional connectivity, suggesting structurally-mediated functional dysconnectivity in TLE.[13]

The focus on individual seed regions or particular networks has so far precluded an integrative view on intrinsic functional network anomalies in TLE, and specifically their associations to underlying perturbations of cortical morphology and microstructure. To fill this gap, we developed a novel rs-fMRI paradigm that systematically profiled intrinsic functional connections across the entire cortical mantle. Our approach combined conventional functional connectomics with a brain-wide geodesic distance mapping technique to estimate connectivity length distributions of any given cortical area, and thus, to draw specific inferences on the balance of short- and long-range connectivity in TLE. Our macroscale connectivity analysis allowed us to assess mechanisms suggested by prior experimental research in models of limbic epilepsy, which posit that aberrant local connectivity and simultaneous deafferentation of long-range connections may form

topologically isolated excitatory circuits that ultimately contribute to recurrent seizure activity.[14, 15] To furthermore assess structural underpinnings of cortex-wide functional connectome reconfigurations, we examined point-wise associations between connectivity distance shifts and MRI measures of cortical morphology and superficial white matter microstructure. Finally, as all patients in our drug-resistant TLE cohort also underwent anterior temporal lobectomy after our imaging investigations, we harnessed machine learning techniques to identify network signatures relevant for post-surgical outcome prognosis. Of note, all patients underwent additional post-surgical imaging, allowing cross-referencing of pre-surgical connectome markers with the extent of the surgical cavity on an individual basis.

MATERIALS AND METHODS

Participants

We studied a consecutive cohort of 30 drug-resistant unilateral TLE patients (15 males, mean±SD=26.9±8.7 years). Patients were diagnosed according to the classification of the International League Against Epilepsy (ILAE) based on a comprehensive examination that includes clinical history, seizure semiology, continuous video-EEG telemetry recordings, neuroimaging, and neuropsychology. Twenty patients had a right-sided seizure focus and ten a left-sided focus. Patients had a mean±SD duration of epilepsy of 11.4±7.9 years (range=2–356 months). No patient had a mass lesion (malformations of cortical development, tumor, vascular malformations) or a history of traumatic brain injury or encephalitis.

Our consecutive patient cohort was selected from a larger patient group, and met the following inclusion criteria: (*i*) patients underwent anterior temporal lobectomy as a treatment of their seizures at Jinling Hospital between August 2008 to April 2017 (mean±SD of 4.3±5.7 months, range=0.1–29 months after our imaging investigations), (*ii*) patients had a research-dedicated high-resolution 3T MRI before surgery that included anatomical, functional, and diffusion imaging, (*iii*) patients had post-operative histological confirmation of hippocampal sclerosis, (*iv*) patients had post-surgical imaging to confirm the location of the surgical cavity, and (*v*) post-surgical seizure outcome was available and determined according to Engel's modified classification [16] with a follow-up of at least one year after surgery (mean±SD=3.23±2.4, range=1-9 years). Among the included patients, 20 (66%) were seizure-free (Engel-I), while four (17%) showed significant

reductions in seizure frequency (Engel-II), four (17%) showed prolonged seizure-free intervals (Engel-III), and two showed no worthwhile improvement (Engel-IV). Detailed information on the patient cohort is presented in **TABLE 1**. Patients were compared to 57 age- and sex-matched healthy individuals (25 males, mean±SD=25.6±5.9 years) who underwent identical imaging.

This study was approved by Research Ethics Board of Jinling Hospital, Nanjing University School of Medicine, and written informed consent was obtain from all participants.

MRI acquisition

Multimodal MRI data were obtained on a Siemens Trio 3T scanner (Siemens, Erlangen, Germany) and included: (*i*) high-resolution 3D T1-weighted MRI using a magnetization-prepared rapid gradient-echo sequence (*T1w*, repetition time [TR] = 2300 ms, echo time [TE] = 2.98 ms, flip angle = 9º, voxel size = 0.5 × 0.5 × 1 mm^3, field of view [FOV] = 256 × 256 mm^2, 176 slices), (*ii*) resting-state blood-oxygen-level dependent (BOLD) functional MRI using a single-shot, gradient-recalled echo planar imaging sequence (*rs-fMRI*, 255 volumes, TR = 2000 ms, TE = 30 ms, flip angle = 90º, FOV = 240 × 240 mm^2, voxel size = 3.75 × 3.75 × 4 mm^3, 30 slices), and (*iii*) diffusion MRI using a spin echo-based echo planar imaging sequence with 4 b0 images (*dwi*, TR = 6100 ms, TE = 93 ms, flip angle = 90º, FOV = 240 × 240 mm^2, voxel size = 0.94 × 0.94 × 3 mm^3, b-value = 1000 s/mm^2, diffusion directions = 120). During the rs-fMRI acquisition, participants were instructed to keep their eyes closed, to not think of anything in particular, and to stay awake. While every participant underwent T1w and rs-fMRI scans, only a subset of controls underwent diffusion MRI (31/57 controls, 14 males, mean±SD age: 27.3±7.4 years; 30/30 TLE patients). To increase power, the main functional analyses were carried out by comparing the TLE patients against all (*i.e.,* 57/57) controls, whereas analyses involving diffusion-derived measures only included the subset of controls who had DWI data available (*i.e.*, 31/57 controls). Of note, all main analyses were replicated by comparing the patients against these 31 controls (see *Results*).

Data preprocessing

T1w images were deobliqued, reoriented, skull stripped, and submitted to FreeSurfer (v6.0; https://surfer.nmr.mgh.havard.edu/) to extract surface models of the cortical mantle.[17] Subject-specific, vertex-wise maps of cortical thickness were then generated by measuring the Euclidean distance between corresponding pial and white matter vertices.

The rs-fMRI scans were preprocessed using FSL (https://fsl.fmrib.ox.ac.uk/fsl/fslwiki/) and AFNI (https://afni.nimh.nih.gov/afni) and included: removal of the first 4 volumes from each time series to ensure magnetization equilibrium, reorientation, motion correction, skull stripping, spatial smoothing using a 6 mm FWHM Gaussian kernel, grand mean scaling, and detrending. Prior to connectivity analysis, time series were statistically corrected for effects of head motion, white matter signal, and cerebrospinal fluid (CSF) signal. They were also band-pass filtered to 0.01-0.10 Hz. Patients and controls did not differ with respect to head motion (t=0.84, p>0.20) and mean framewise displacement (t=1.24, p>0.11). Following rs-fMRI preprocessing, a boundary-based registration technique[18] mapped the functional time series to each participant's cortical surface and subsequently to a 10k vertices (*i.e.*, surface points) version of the Conte69 human symmetric surface template.

Diffusion MRI data were preprocessed using MRTrix[3] (v0.3.15; http://www.mrtrix.org/) and included correction for susceptibility distortions using FSL TOPUP[19] as well as for motion and eddy currents using FSL EDDY. As in prior work,[5] we generated surfaces probing the white matter ~2 mm beneath the cortical interface to examine diffusion measures along the superficial white matter. Surfaces were derived by systematically contracting the white matter interface along a Laplacian potential field towards the ventricular walls. Diffusion tensor-derived fractional anisotropy (FA) and mean diffusivity (MD), surrogates of fiber architecture and tissue microstructure, were interpolated along these surfaces and mapped to Conte69.

Distance-enriched functional connectivity analyses

Individualized functional connectomes were generated by computing pairwise correlations between all pairs of vertices. For each region within the z-transformed connectome matrices, we retained the top 10% of weighted connections and calculated the average geodesic distance to all other regions in this connectivity profile. The resulting connectivity distance maps recapitulate a given region's geodesic distance to its functionally connected areas within the cortex and, as such, characterize the relationship between physical distance and functional connectivity. In contrast to conventional seed-, community-, or gradient-based functional connectivity analyses, our connectivity distance profile approach provides additional topographic information that can differentiate local from distant projection patterns. Distance maps in patients were z-scored relative to controls and sorted into ipsilateral/contralateral to the focus.[20] As in previous work,[2] surface-

based linear models compared connectivity distance in patients relative to controls using SurfStat,[21] available at http://mica-mni.github.io/surfstat. Findings were corrected for age and sex, as well as for multiple comparisons at a family-wise error (FWE) rate of $p<0.05$.

Post-hoc analyses centered on regions of connectivity distance alterations in TLE furthermore quantified connectivity distance shifts, informed by Harrell-Davis quantile estimators.[22] For statistical significance estimation, we computed 95% bootstrap confidence intervals of the decile-wise differences between controls and TLE, computed across 1000 iterations.

Connectivity distance asymmetry

To assess the utility of our findings for seizure focus lateralization, we repeated the connectivity distance analysis in left and right TLE cohorts independently. Inter-hemispheric asymmetry maps of connectivity distance were also computed for each patient.

$$ASYMMETRY = (ipsilateral - contralateral) / ((ipsilateral + contralateral) / 2)$$

Using surface-based paired *t*-tests, we then compared ipsilateral *vs*. contralateral connectivity distance profiles in TLE.

Rich club, community-, and gradient-based stratification

A series of analyses contextualized our findings with respect to whole-brain network topology.

a) Rich club. The 'rich club' refers to a network core consisting of high-degree and densely interconnected *hub regions*.[23] In contrast to locally-connected peripheral nodes, it accumulates most long-range connections, plays an important role in network communication, and is more vulnerable to pathological perturbations. To assess connectivity distance reductions with respect to rich club taxonomy, we computed the weighted rich club coefficient $\phi^w(k)$ across the range of possible degrees. We normalized this coefficient relative to 1000 randomly-generated networks with similar degree and weight properties as the original network.[24] Nodes with degree $k \geq 1700$ were characterized as rich club nodes and those with $k < 1700$ as peripheral. To ensure that findings were not biased by the choice of k, analyses were repeated across different thresholds within a 'rich club regime', comprising normalized $\phi^w(k)$ values between $k \geq 1500$ to 1900. Connections were classified into rich club connections (*i.e.*, between rich club nodes), feeder connections (*i.e.*,

between rich club and peripheral nodes), and local connections (*i.e.*, between peripheral nodes). Patient-specific vertex-wise connectivity distance findings, *z*-scored to controls, were then averaged across each of the rich club, feeder, and local connections, and Cohen's *d* effect sizes were estimated per class.

b) Communities and functional gradients. We stratified distance alterations based on a well-established functional atlas of seven canonical resting-state networks.[25] In contrast to decomposing the brain into discrete networks, recent work has suggested that the human functional connectome can also be characterized by a principal gradient describing a smooth transition that runs from unimodal sensory systems towards higher-order transmodal networks, such as the default mode and frontoparietal network.[26] Using a previously described approach,[26] the connectome gradient was computed using 100 subjects from the Human Connectome Project and subsequently surface registered to the 10k downsampled Conte69 template. As in previous connectome gradient profiling analyses,[27] we partitioned the gradient into 20 bins, ranging from unimodal regions (1st bin) to higher-order/transmodal areas situated at the top of the processing hierarchy (20th bin), and calculated mean vertex-wise connectivity distance at each bin. Patients and controls were compared using two-sample *t*-tests at each community and at each gradient bin, respectively. Findings were corrected for multiple comparisons using False Discovery Rate (FDR) procedures.

Relation to cortical morphology and microstructure

To examine structural underpinnings of functional connectivity distance shifts, we repeated the above analyses while controlling for effects of cortical thickness and superficial white matter microstructure, respectively.

a) Cortical morphology. Lateralization and disease duration have been shown to contribute to cortical thinning in TLE;[28] however, effects of atrophy on functional connectivity alterations remain relatively underexplored. Surface-based linear models first compared cortical thickness in TLE compared to controls while controlling for age and sex. We also assessed functional connectivity distance alterations in TLE *vs.* controls while controlling for cortical thickness alterations at each vertex to investigate shifts in the connectivity distance distribution in TLE above and beyond effects of cortical atrophy.

b) Superficial white matter microstructure. The superficial white matter immediately beneath the cortex harbors termination zones of long-range tracts and short-range, cortico-cortical U-fibers.[29] This compartment is therefore ideal to study the interplay between cortical microstructure, connectivity, and function.[5] Surface-based linear models compared diffusion MRI-derived superficial white matter microstructure in TLE *vs.* controls, controlling for age and sex. As in *a*), we compared functional connectivity distance between groups while also controlling for vertex-wise diffusion parameters to investigate functional connectivity anomalies in TLE above and beyond superficial white matter perturbations.

Association to surgical outcome

Recent neuroimaging evidence supports an increasing role of structural and functional network modeling in informing clinical practice.[30] While prior research has trained classification algorithms using isolated structural and diffusion markers to predict post-surgical seizure freedom,[6, 31] the utility of functional connectivity in this context remains underexplored. Here, we used a supervised pattern learning paradigm to evaluate whether functional connectivity distance shifts can predict post-surgical seizure outcome in individual patients. Specifically, we build learners discriminating seizure-free (Engel I) from non-seizure-free (Engel II-IV) patients. To minimize overfitting, a two-step dimensionality reduction was performed on individual-level connectivity distance maps. Maps were first parcellated using the Desikan-Killiany atlas, yielding 68 features for each individual map, and subsequently fed into a principal component analysis to generate orthogonal components. These components were submitted to a L2-regularized logistic regression models. Training and performance evaluation employed nested 5-fold cross-validation with 100 iterations to allow for unbiased and conservative performance assessment of previously unseen cases. Statistical performance of the model was assessed using 1000 permutation tests with randomly shuffled surgical outcome labels. To index feature importance across cortical regions, we multiplied logistic regression coefficients by principal component scores and subsequently mapped them to the surface template, with positive feature weight values being predictive of seizure-free outcome and negative values being predictive of non-seizure-free outcome.

To combine pre-operative feature data with individualized surgical data, we related the feature learning derived weights to surgical resection cavities in individual patients. To this end, we automatically segmented post-surgical cavities by registering both pre- and post-operative T1w

images to the MNI152 standard template through linear transformations and subsequently subtracting the post-operative scan from the pre-operative scan. Segmented cavities were visually inspected and manually edited to ensure that the extent of the resection cavity was identified correctly. Patient-specific cavities were then mapped to cortical surfaces, registered to the Conte69 template, and a consensus label was generated as defined by the union of all segmentations. To associate resection information with the statistical pattern learning results, we computed classifier-determined weights within and outside the patient-specific cavity masks.

RESULTS

Connectivity distance reductions in TLE

In controls, we observed marked variations in average connectivity distance from a given region to its functionally connected areas across the cortical mantle, with transmodal networks showing longest distances and sensory cortices showing shortest distances (**FIGURE 1A)**. Notably, TLE patients demonstrated marked reductions relative to controls (**FIGURE 1B)** in a bilateral network encompassing lateral temporo-limbic cortices (ipsilateral: $p<0.001$; contralateral: $p=0.05$; *FWE-corrected*) and dorsomedial prefrontal regions (ipsilateral: $p=0.09$; contralateral: $p<0.005$; *FWE-corrected*), as well as contralaterally in ventromedial prefrontal cortex ($p<0.05$; *FWE-corrected*) and ipsilaterally in inferior frontal gyrus ($p=0.06$; *FWE-corrected*). Density distribution of every vertex within these three significant clusters, sorted by the average geodesic distance of that vertex to its functionally connected areas, indicated that connectivity distance changes related to concurrent increases in short-range and decreases in long-range connections in TLE (**FIGURE 1C**).

Dominant patterns of connectivity distance reductions involving the ipsilateral temporal cortex were observed in left and right TLE cohorts independently ($p<0.001$; *FWE-corrected*, **FIGURE 2A**). Similarly, analysis of within-patient asymmetry maps revealed pronounced connectivity distance reductions in ipsilateral anterolateral and anteromedial temporal regions ($p<0.001$; *FWE-corrected*, **FIGURE 2B**). Individual analyses in this cluster confirmed that the vast majority (23/30; 77%) of patients indeed showed dominant ipsilateral compared to contralateral reductions.

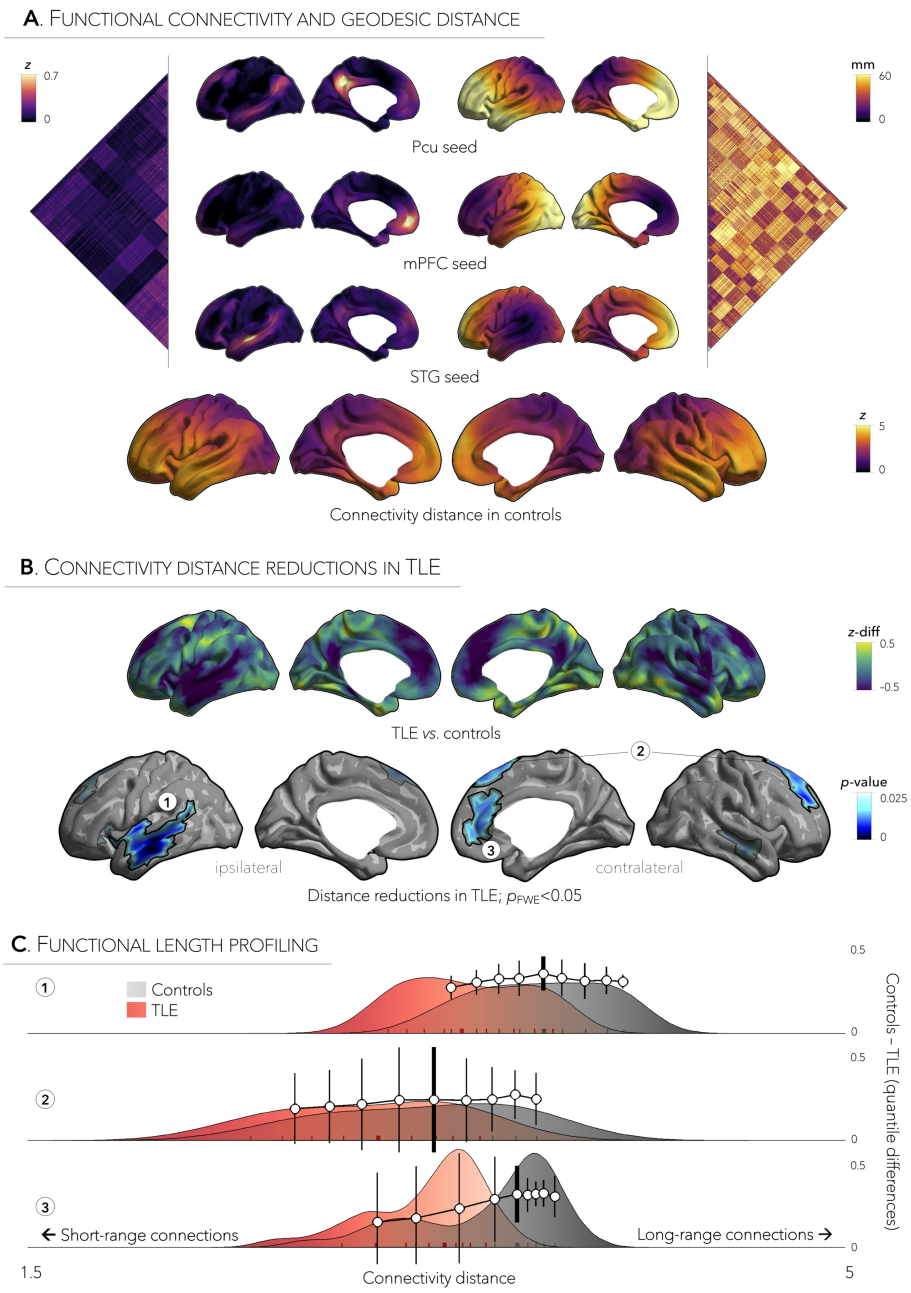

FIGURE 1. Connectivity distance reductions in temporal lobe epilepsy (TLE). a | Functional connectivity and geodesic distance profiles are displayed for three exemplary regions: precuneus (Pcu; *top*), medial prefrontal cortex (mPFC; *middle*), and superior temporal gyrus (STG; *bottom*). Cortex-wide variations in connectivity distance in healthy controls, with transmodal networks showing longest distances and sensory and motor cortices the shortest. b | Relative to controls, TLE patients showed marked connectivity distance reductions in bilateral temporal and insular cortices and dorsomedial prefrontal regions, as well as contralateral ventromedial prefrontal cortex, and ipsilateral inferior frontal gyrus. Significant clusters of connectivity reductions are numbered 1–3. Trends of connectivity distance reductions are shown in semi-transparent. c | Connectivity reductions in these clusters were driven by concurrent increases in short-range and decreases in long-range connections in TLE. Shift functions are superimposed onto each distribution and illustrate by how much connectivity distance profiles are shifted in TLE (red) relative to controls (grey). Vertical lines along this function indicate the 95% bootstrap confidence interval for each decile difference (Controls – TLE). Shorter lines at the bottom of each distribution mark the deciles for each group; thicker lines represent the median.

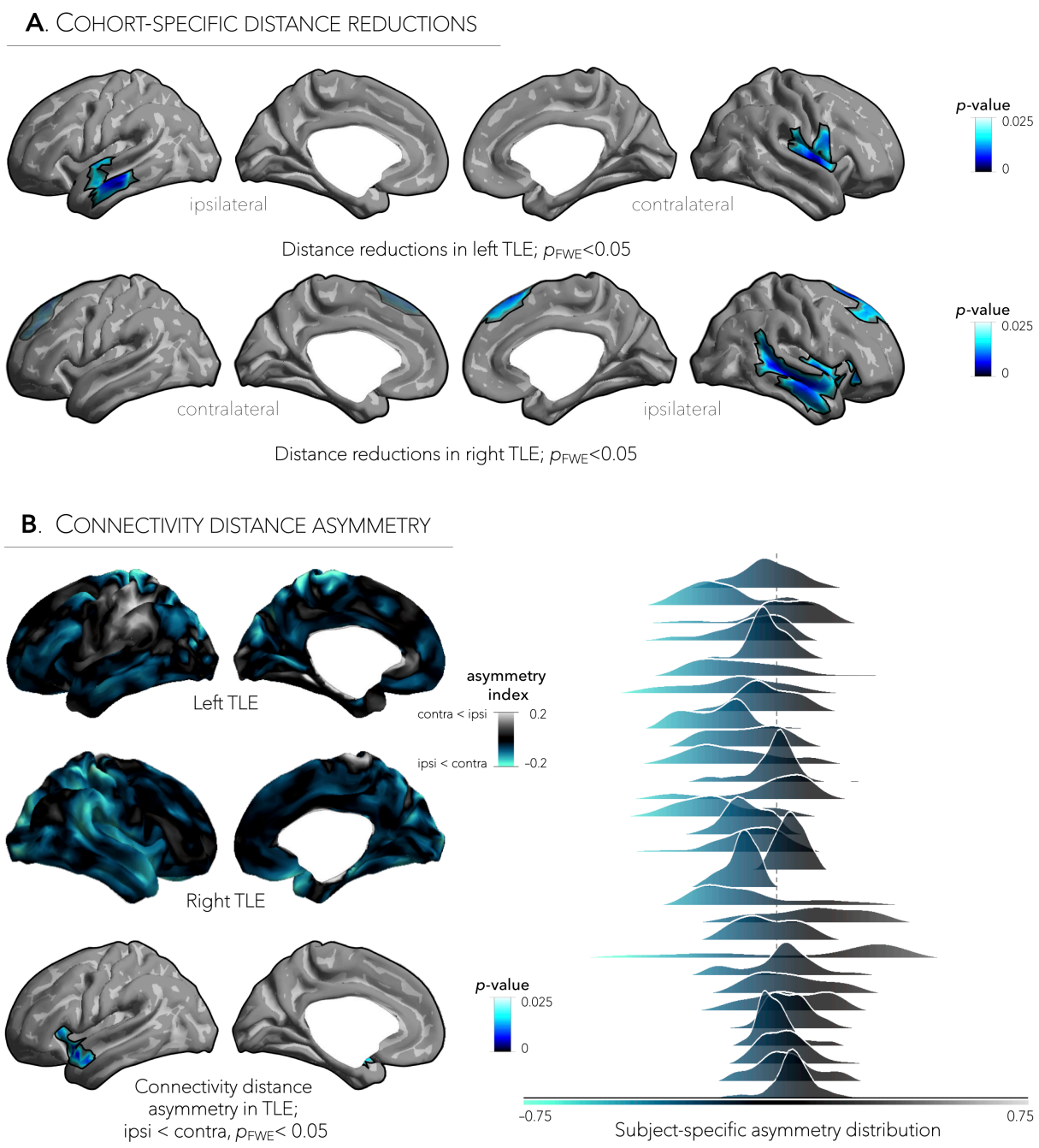

FIGURE 2. **Connectivity distance asymmetry as a lateralizing sign in TLE**. **a |** Dominant patterns of connectivity reductions in left and right TLE encompassed an ipsilateral network involving temporal and insular cortices. Trends of connectivity distance reductions are shown in semi-transparent. **b |** Asymmetry maps comparing connectivity distance in ipsilateral *vs*. contralateral hemispheres in left and right TLE cohorts showed reductions in ipsilateral anterior temporal regions, and subject-specific asymmetry values within this cluster showed consistent asymmetry in 77% of patients.

Several connectome-wide analyses contextualized the TLE-related connectivity distance reduction within key features of large-scale network topology. Considering rich club organization [23], strongest reductions in TLE were observed among densely interconnected rich club nodes (**FIGURE 3A**), indicating higher susceptibility of hub regions to connectivity contractions. As similar finding was also suggested by community-based stratification [25], showing strongest effects in the default-mode network (p<0.025; *FDR-corrected*, **FIGURE 3B**). Similarly, connectome topographic profiling located maximal effects at the transmodal apex of the adult connectome gradient [26] (p<0.025; *FDR-corrected*, **FIGURE 3C**).

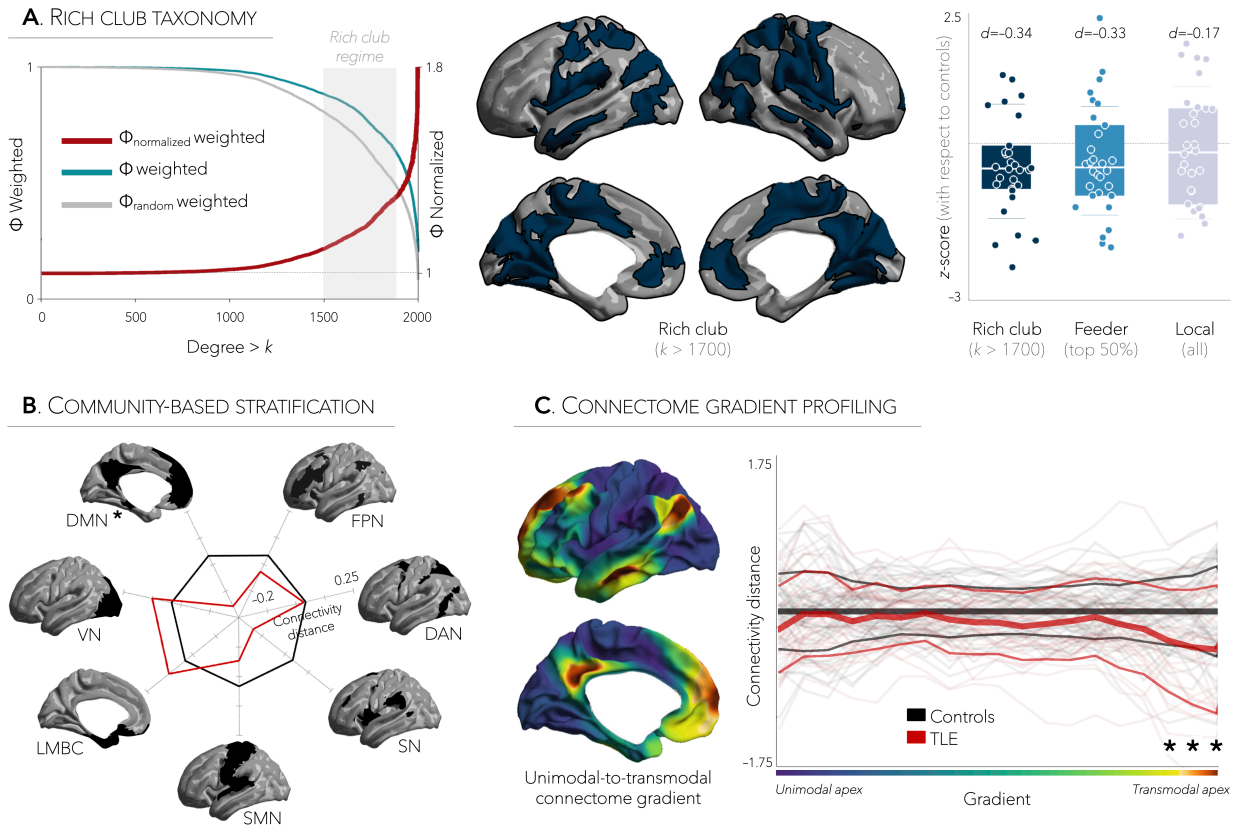

FIGURE 3. **Connectivity distance reductions in TLE co-localize with high-degree, transmodal networks**. **a |** The distribution of rich club nodes was mapped onto the surface template and Cohen's *d* effect sizes indicated that connectivity distance reductions co-localized strongly with rich club (rich club–rich club) and feeder (rich club–local) connections. **b |** Stratification of the functional connectome into seven canonical resting-state networks [25] revealed that TLE patients have preferential connectivity reductions in default-mode (DMN) network. **c |** Similarly, connectivity reductions in TLE closely co-localized with the transmodal apex of the adult connectome gradient [26], which differentiates between unimodal, sensory and higher-order, transmodal systems. * = p<0.025; *FDR-corrected*.

Connectivity reductions are mediated by microstructural damage

Compared to controls, patients presented with cortical thinning across bilateral premotor, superior frontal, and paracentral cortices (p<0.001; *FWE-corrected*), ipsilateral temporal pole extending into mesiotemporal regions (p<0.001; *FWE-corrected*, **FIGURE 4B**). Spatial comparison between areas of cortical atrophy and patterns of connectivity distance reductions revealed minimal overlap (Dice=0.02); furthermore, findings of connectivity distance reductions remained robust after correcting for cortical thickness, suggesting independence from morphological alterations.

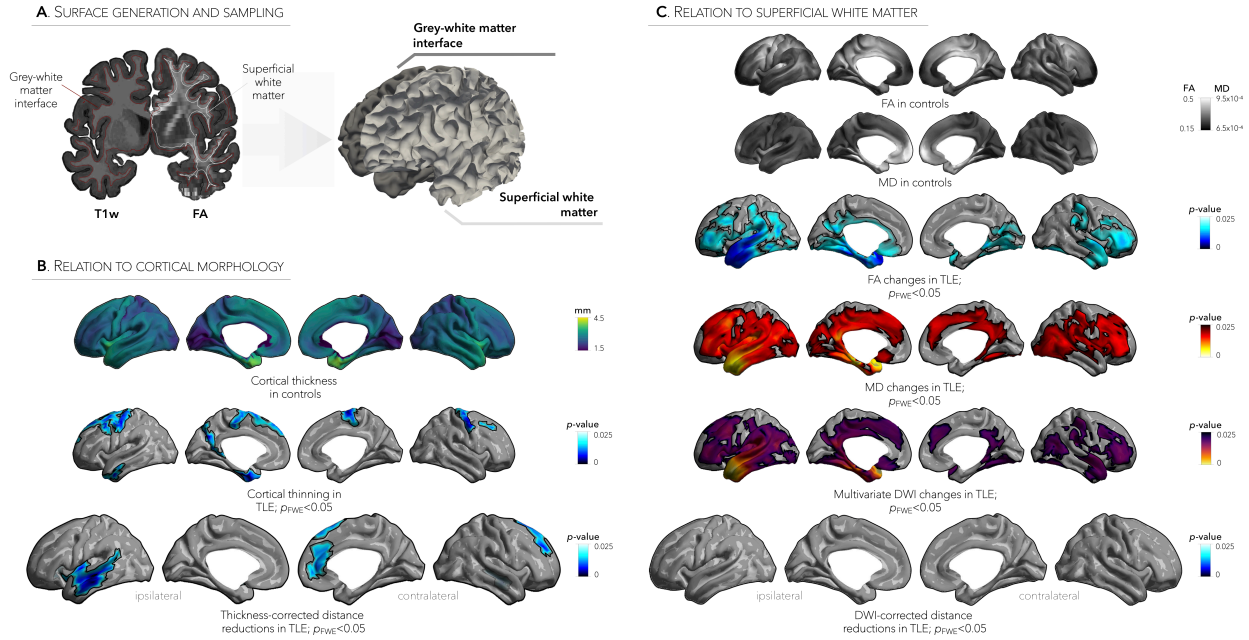

FIGURE 4. **Microstructural damage mediates connectivity distance reductions**. **a |** Cortical thickness was measured at each vertex as the Euclidean distance between white and pial surfaces, whereas fractional anisotropy (FA) and mean diffusivity (MD) were sampled along superficial white matter surfaces generated 2 mm below the grey-white matter interface. **b |** Patterns of cortical thinning differed from that of functional connectivity reductions in TLE, suggesting that shifts in the connectivity distance distribution occurred independently of cortical atrophy. **c |** Repeating the connectivity distance analysis while controlling for superficial white matter effects revealed no significant changes in TLE compared to controls, suggesting a mediatory role of microstructural damage in functional distance reductions.

We also observed extensive superficial white matter diffusion alterations in TLE relative to controls, albeit in a different spatial distribution as cortical thickness reductions. Marked superficial white matter alterations, characterized by reduced FA and increased MD, were located in the ipsilateral temporal pole (p<0.001; *FWE-corrected*), but also extended centrifugally to bilateral frontal, temporal, and occipital cortices (p<0.05; *FWE-corrected*; **FIGURE 4C**). Overlaps with functional changes were modest (*Dice=0.12*). Moreover, the effect size of connectivity

distance reductions in TLE was markedly reduced when repeating analyses while controlling for superficial white matter metrics (effect size reductions up to 45% across clusters of findings; with strongest reductions in ipsilateral temporal regions), suggesting a mediatory role of microstructural damage in functional distance reductions.

Associations to post-surgical seizure recurrence

A supervised pattern learning paradigm evaluated whether post-surgical seizure freedom imparts distinct signatures on connectivity distance profiles. Dimensionality reduction of the connectivity distance maps yielded 24 principal components explaining 98.7% in variance. Using 5-fold cross-validations, we found that connectivity distance predicted surgical outcome (seizure-free *vs*. non-seizure-free) at a mean±SD accuracy of 75±4% (100 iterations). Permutation tests with 1000 randomly shuffled outcome labels indicated that performance exceeded chance levels ($p<0.05$). Features associated with seizure freedom included connectivity distance reductions in ipsilateral default-mode nodes (medial and lateral ventral prefrontal cortex, angular gyrus, posterior superior temporal gyrus) as well as contralateral temporo-insular cortices. Conversely, connectivity distance reductions associated with seizure recurrence were predominantly located contralaterally in mesial temporal, orbitofrontal, visual, and centro-parietal cortices, as well as in ipsilateral frontopolar cortex (**FIGURE 5A**). Analyzing classifier weights inside/outside the cavity indicated that connectivity distance reductions inside the cavity were associated with seizure freedom, while reductions outside the cavity, specifically in contralateral regions, predicted seizure recurrence. This shift was consistent across patients, and highly significant (paired *t*-test, $p<0.001$; **FIGURE 5B**).

Analysis of list-complete data

As only a subset of control participants had DWI data available (*i.e.*, 37/57), we performed a list-complete control analysis to ensure reproducibility of our functional connectivity distance findings. Accordingly, we repeated the above analyses comparing the patients to the 37 of controls that underwent diffusion MRI, and observed virtually identical findings as in our main analyses. **(SUPPLEMENTARY FIGURES 1 AND 2).**

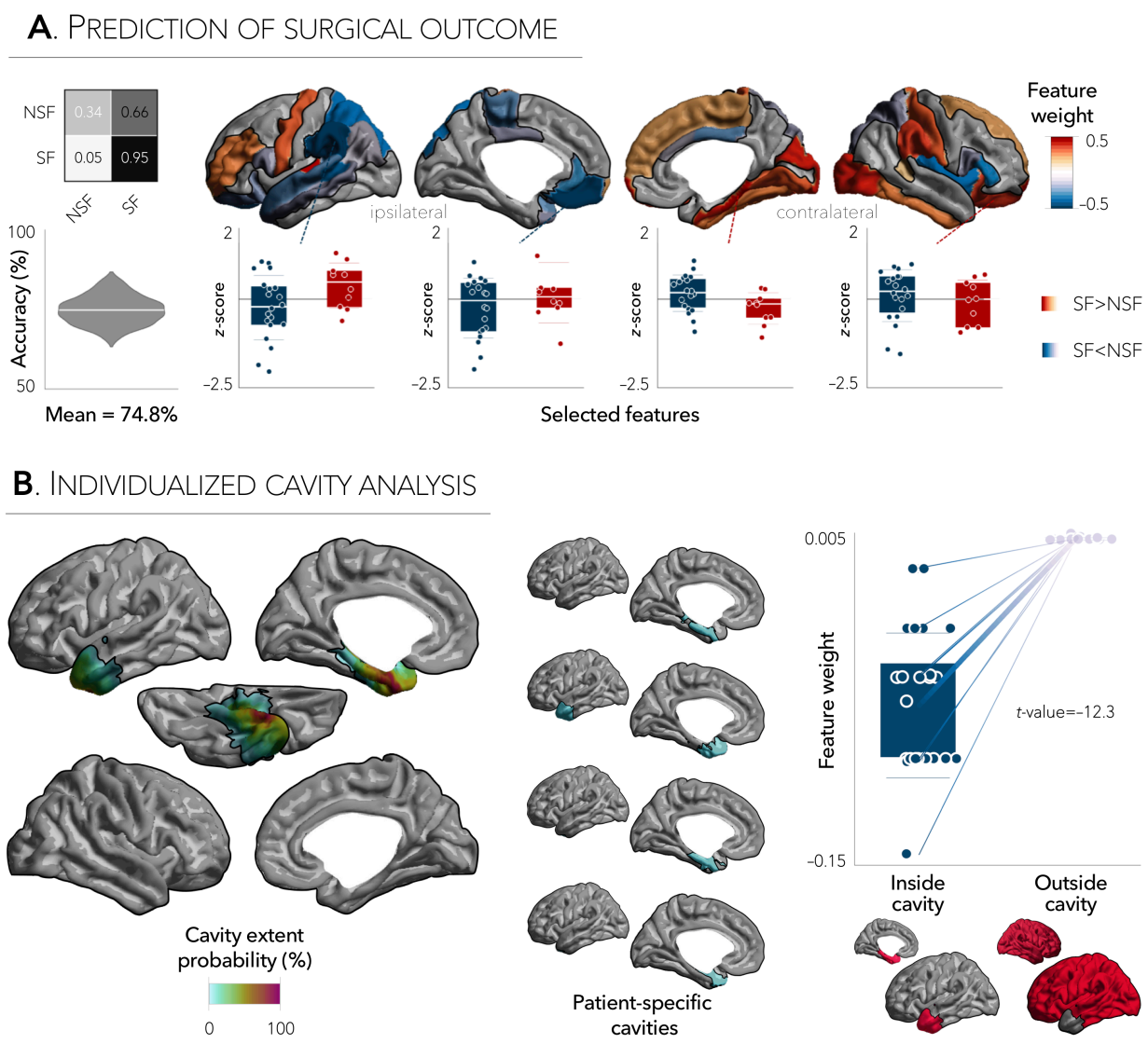

FIGURE 5. **Connectivity distance signature of surgical outcome**. **a |** A supervised learning algorithm was trained on functional connectivity distance data to predict surgical outcome in patients (seizure-free; SF *vs*. non-seizure-free; NSF) and achieved 74.8% accuracy. Confusion matrix summarizing the model's performance is displayed in inset (values range from 0 to 1). Most important features (top and bottom 25%) are mapped to the cortical surface while boxplots for four exemplary regions depict mean connectivity distance values as a function of group. **b |** Cavity extent probability across patients, and individual cavity maps for a subset of patients are projected onto the surface template. Seizure free patients showed more marked connectivity distance reductions in ipsilateral regions, whereas those with persistent seizures were characterized by distance reductions in regions contralateral to the surgical cavity.

DISCUSSION

Motivated by prior experimental and histopathological research suggesting a link between recurrent spontaneous seizures and topological isolation of local circuits,[15, 32] the current work examined the balance between short and long-range functional connections in TLE. Our analysis was centered on a novel *in vivo* approach that integrated shifts in the relationship between resting-state functional connectivity and physical distance between areas across the cortical mantle. Comparing a cohort of drug-resistant TLE patients to controls, we observed marked reductions in temporo-limbic and dorsomedial prefrontal cortices in TLE. Subsequently mapping the balance between local and distant projection patterns, connectivity contractions in TLE were found to be primarily driven by increases in short-range functional connections and concomitant decreases in long-range connections, specifically in temporo-limbic areas. When exploring the role of co-occurring morphological and microstructural perturbations, as previously reported in this condition,[3, 5, 33] we observed that connectivity reductions were independent of temporal and fronto-central cortical thinning but were found to be mediated by a centrifugal pattern of superficial white matter alterations stemming from the mesiotemporal epicenter. Notably, a regularized supervised learner with conservative 5-fold cross-validation identified salient connectivity distance features that predicted post-surgical seizure recurrence with 75% accuracy, suggesting prognostic utility when feeding distance-enriched connectome profiling maps into machine learning algorithms. Collectively, our findings provide novel *in vivo* evidence for topological isolation as a potential disease mechanism of TLE, and support promising clinical benefits of combining connectomic data with physically-grounded information.

Our study harnessed rs-fMRI, a non-invasive window to probe intrinsic functional networks in a highly reproducible and individualized manner. Conventional rs-fMRI connectivity analyses generally focus on *a-priori* defined seeds or decompose the brain into discrete communities using unsupervised compression and clustering methods. Contrastingly, an appealing feature of our analytical framework lies in the continuous profiling of connectivity distances along the folded cortical sheet. Mirroring previously reported maps of cortical distance in healthy individuals,[34] we observed marked inter-areal variations in the average physical distance of a region's functional connections. Indeed, connectivity distances were shortest in visual and sensorimotor networks, communities known for their predominantly locally clustered cortico-cortical connectivity

organization, and longest in transmodal association areas performing integrative functions known to be instantiated by distributed systems, such as the default-mode, frontoparietal, and limbic networks. When compared to controls, TLE patients presented with a significant loss of long-range communication pathways emanating from bilateral temporo-insular cortices, a finding consistent with covariance analyses focused on the mesiotemporal circuitry showing topologically isolated networks in drug-resistant TLE.[35] Importantly, assessing left and right TLE patients separately yielded dominant ipsilateral temporo-limbic effects and, as such, confirmed robustness of our findings. At the individual level, connectivity distance reductions restricted to the anterior temporal cortex showed consistent asymmetry in 77% of patients, supporting potential clinical benefits of our approach for pre-operative focus lateralization. The close co-localization of functional connectivity anomalies with the anterior temporal lobe surgical cavity further motivates future work to examine associations between our imaging-derived connectome measures and neurophysiological markers that may index epileptogenicity, notably abnormal rates of high-frequency oscillations and content of low-voltage fast activity at ictal EEG seizure-onset.[36, 37]

In addition to macroscale functional perturbations, a growing body of neuroimaging findings has shown widespread effects of TLE on brain structure.[2] By mapping the connectivity distance of every region along the continuous cortical sheet, our framework offered a reference frame to reconcile macroscale function with MRI-derived measures of morphology and microstructure. Cortical thickness reductions in our TLE cohort followed a bilateral temporal and fronto-central spatial topography, a finding in agreement with previous cross-sectional[2-4] and longitudinal imaging studies,[28] along with recent meta-analytical synthesis performed across 19 international sites.[38] In contrast to widespread cortical atrophy, microstructural perturbations, quantified here using a previously developed surface-based approach to profile superficial white matter diffusivity,[5] followed a specific temporo-limbic spatial pattern with dominant effects ipsilateral to the focus. Importantly, by integrating structural and functional measures in a point-wise manner across the entire cortical landscape, we directly examined interactions between distance-enriched functional organization and morphological as well microstructural substrates. Previous studies relating structure and function in the healthy connectome have generally yielded stronger correspondence of functional interactions with structural connectivity estimated from diffusion imaging than with T1w-derived estimates of cortical morphology.[39] Similarly, the lack of a clear association between TLE-related atrophy and distance-enriched functional shifts in the current

study suggests that cortical thinning may relate to pathophysiological processes underlying seizure-induced damage.[28] On the other hand, functional connectivity findings strongly overlapped with white matter changes in the temporo-limbic circuitry, supporting a mediatory role of this compartment in cortico-cortical functional anomalies characteristic of drug-resistant TLE. Such findings are also reported when profiling specific deep white fiber tracts[40] and surface-based superficial white matter markers,[5] with anomalies tapering off with increasing distance from the affected mesiotemporal lobe. In addition to their spatial resemblance to the agranular/dysgranuar limbic territory, white matter changes have also been more consistently related to the severity of hippocampal pathology than grey matter thinning, and may therefore represent a connectome-level cascade secondary to mesiotemporal pathology in TLE.[41] By consolidating previously reported disease effects from multiple spatial scales with distance-enriched functional profiles, our study offers non-invasive insights into the mechanisms by which mesiotemporal anomalies may ultimately propagate to whole-brain functional networks in TLE.[42]

Our surface-based findings, particularly the reductions in long-range connectivity together with increases in local connections in temporo-limbic circuits may provide a physical mechanism underlying previous topological findings reporting increased path length and clustering in TLE using graph theoretical analysis of connectivity data obtained from various modalities.[43] These changes were previously labelled as network regularization, and frequently observed in experimental models of cortical epilepsy[44] as well as in patients with drug-resistant focal epilepsy.[43] While several network configurations may promote spontaneous seizures,[45] spatial compactness of local circuits has been suggested as a plausible network-level mechanism that tilts the balance towards epileptogenesis by facilitating recurrent activity and local oscillations.[15] Prior EEG/SEEG studies have indeed reported network regularization at seizure onset, a configuration that shifts towards a globally integrated process as the seizure progresses, eventually reaching a random configuration upon seizure termination.[46] Additional intracranial connectivity measures have also revealed increased connectivity in epileptogenic networks when compared to regions outside of the epileptogenic zone.[47] To further explore computational mechanisms of seizure dynamics, it has been speculated that local clusters of neurons may isolate themselves from the rest of the network, likely through an imbalance between local and distant connections, a mechanism described as "network tightening".[48] Under this account, however, functional isolation of the seizure-onset zone was speculated to play a role in annihilating epileptogenic activity and,

as such, may represent a potential compensatory mechanism through which locally confined, seizure-related activity is prevented from spreading.

We close by highlighting that our measures were ~75% accurate in predicting post-surgical seizure outcome at a mean of three years post-operative follow-up when using a supervised pattern learning paradigm with 5-fold cross-validation. As expected, dominant connectivity distance reductions in ipsilateral regions related to better outcomes, while signatures predicting seizure recurrence encompassed extra-temporal and contralateral regions, a finding that parallels predictors of surgical failure seen at the level of morphological measures[49] and diffusion MRI metrics.[31] These findings were strengthened due to our inclusion criteria, which required post-surgical MRI and histological confirmation of the resected cavity in all patients. In fact, this approach revealed that the balance of anomalies inside *vs*. outside the cavity served as a key driver for outcome prognosis. Additional strengths of our approach rely on the use of conservative cross-validation for training and validation as well as relatively long post-surgical follow-up times averaging three years. Nevertheless, in light of prior work suggesting the possibility of seizure recurrence at longer follow-up times in post-surgical patients that were initially considered seizure-free [50], we cannot rule out potential sources of uncertainty in the surgical outcome labels used in our study. Future studies may also better characterize the generalizability and predictive power of our findings in other prevalent drug-resistant focal epilepsies related to malformations of cortical development, notably focal cortical dysplasia with subtle structural imaging signs. Large-scale initiatives such as ENIGMA-epilepsy[38] have demonstrated that it is possible to aggregate multimodal neuroimaging metrics and clinical information, and to coordinate analytical strategies across sites. This concerted push towards openly available, large-scale consortia in the epilepsy community will be instrumental for the validation and dissemination of biomarkers and novel approaches such as the one developed in the current study.

ACKNOWLEDGEMENTS

SL acknowledges funding from Fonds de la Recherche du Québec – Santé (FRQ-S) and the Canadian Institutes of Health Research (CIHR). RvdW receives support from a Savoy Foundation studentship. BF receives funding from FRQ-S (Chercheur-Boursier clinician Junior 2). AB and NB were supported by FRQ-S and CIHR (MOP-57840, MOP-123520). ZZ was supported by National Science Foundation of China (NSFC: 81422022; 863 project: 2014BAI04B05 and 2015AA020505) and China Postdoctoral Science Foundation (2016M603064). BCB acknowledges research funding from the SickKids Foundation (NI17-039), the National Sciences and Engineering Research Council of Canada (NSERC; Discovery-1304413), CIHR (FDN-154298), Azrieli Center for Autism Research (ACAR), an MNI-Cambridge collaboration grant, and salary support from FRQ-S (Chercheur-Boursier).

AUTHOR CONTRIBUTIONS

BCB, ZZ, and SL designed the study. SL, RvdW, and YW carried out the image processing and network analysis. SL and BCB wrote the paper, and revised it with AB, NB, ZZ, ZW, DS, and BF.

POTENTIAL CONFLICTS OF INTEREST

The authors report no conflicts of interest.

REFERENCES

1. Bernhardt BC, Bonilha L, Gross DW. Network analysis for a network disorder: The emerging role of graph theory in the study of epilepsy. Epilepsy Behav 2015;50:162-170.

2. Bernhardt BC, Bernasconi N, Concha L, Bernasconi A. Cortical thickness analysis in temporal lobe epilepsy: reproducibility and relation to outcome. Neurology 2010;74:1776-1784.

3. McDonald CR, Hagler DJ, Jr., Ahmadi ME, et al. Regional neocortical thinning in mesial temporal lobe epilepsy. Epilepsia 2008;49:794-803.

4. Lin JJ, Salamon N, Lee AD, et al. Reduced neocortical thickness and complexity mapped in mesial temporal lobe epilepsy with hippocampal sclerosis. Cereb Cortex 2007;17:2007-2018.

5. Liu M, Bernhardt BC, Hong SJ, Caldairou B, Bernasconi A, Bernasconi N. The superficial white matter in temporal lobe epilepsy: a key link between structural and functional network disruptions. Brain 2016;139:2431-2440.

6. Bonilha L, Helpern JA, Sainju R, et al. Presurgical connectome and postsurgical seizure control in temporal lobe epilepsy. Neurology 2013;81:1704-1710.

7. Liao W, Zhang Z, Pan Z, et al. Altered functional connectivity and small-world in mesial temporal lobe epilepsy. PLoS One 2010;5:e8525.

8. He X, Doucet GE, Sperling M, Sharan A, Tracy JI. Reduced thalamocortical functional connectivity in temporal lobe epilepsy. Epilepsia 2015;56:1571-1579.

9. Bettus G, Guedj E, Joyeux F, et al. Decreased basal fMRI functional connectivity in epileptogenic networks and contralateral compensatory mechanisms. Hum Brain Mapp 2009;30:1580-1591.

10. Morgan VL, Rogers BP, Sonmezturk HH, Gore JC, Abou-Khalil B. Cross hippocampal influence in mesial temporal lobe epilepsy measured with high temporal resolution functional magnetic resonance imaging. Epilepsia 2011;52:1741-1749.

11. Maccotta L, He BJ, Snyder AZ, et al. Impaired and facilitated functional networks in temporal lobe epilepsy. NeuroImage Clinical 2013;2:862-872.

12. Pittau F, Grova C, Moeller F, Dubeau F, Gotman J. Patterns of altered functional connectivity in mesial temporal lobe epilepsy. Epilepsia 2012;53:1013-1023.

13. Bernhardt BC, Bernasconi A, Liu M, et al. The spectrum of structural and functional imaging abnormalities in temporal lobe epilepsy. Ann Neurol 2016;80:142-153.

14. Knopp A, Kivi A, Wozny C, Heinemann U, Behr J. Cellular and network properties of the subiculum in the pilocarpine model of temporal lobe epilepsy. J Comp Neurol 2005;483:476-488.

15. Sharma AK, Reams RY, Jordan WH, Miller MA, Thacker HL, Snyder PW. Mesial temporal lobe epilepsy: pathogenesis, induced rodent models and lesions. Toxicol Pathol 2007;35:984-999.

16. Engel Jr JJStote. Outcome with respect to epileptic seizures. 1993:609-621.

17. Dale AM, Fischl B, Sereno MI. Cortical surface-based analysis. I. Segmentation and surface reconstruction. Neuroimage 1999;9:179-194.

18. Greve DN, Fischl B. Accurate and robust brain image alignment using boundary-based registration. Neuroimage 2009;48:63-72.

19. Andersson JL, Skare S, Ashburner J. How to correct susceptibility distortions in spin-echo echo-planar images: application to diffusion tensor imaging. Neuroimage 2003;20:870-888.

20. Liu M, Bernhardt BC, Bernasconi A, Bernasconi N. Gray matter structural compromise is equally distributed in left and right temporal lobe epilepsy. Human brain mapping 2016;37:515-524.

21. Worsley KJ, Taylor J, Carbonell F, et al. A Matlab toolbox for the statistical analysis of univariate and multivariate surface and volumetric data using linear mixed effects models and random field theory. NeuroImage Organisation for Human Brain Mapping 2009 Annual Meeting; 2009: S102.

22. Harrell FE, Davis C. A new distribution-free quantile estimator. Biometrika 1982;69:635-640.

23. van den Heuvel MP, Sporns O. Rich-club organization of the human connectome. J Neurosci 2011;31:15775-15786.

24. Rubinov M, Sporns O. Complex network measures of brain connectivity: uses and interpretations. Neuroimage 2010;52:1059-1069.

25. Yeo BT, Krienen FM, Sepulcre J, et al. The organization of the human cerebral cortex estimated by intrinsic functional connectivity. J Neurophysiol 2011;106:1125-1165.

26. Margulies DS, Ghosh SS, Goulas A, et al. Situating the default-mode network along a principal gradient of macroscale cortical organization. Proc Natl Acad Sci U S A 2016;113:12574-12579.

27. Murphy C, Jefferies E, Rueschemeyer SA, et al. Distant from input: Evidence of regions within the default mode network supporting perceptually-decoupled and conceptually-guided cognition. Neuroimage 2018;171:393-401.

28. Coan AC, Appenzeller S, Bonilha L, Li LM, Cendes F. Seizure frequency and lateralization affect progression of atrophy in temporal lobe epilepsy. Neurology 2009;73:834-842.

29. Schmahmann J, Pandya D. Fiber pathways of the brain: OUP USA, 2009.

30. Engel J, Jr., Thompson PM, Stern JM, Staba RJ, Bragin A, Mody I. Connectomics and epilepsy. Curr Opin Neurol 2013;26:186-194.

31. Gleichgerrcht E, Munsell B, Bhatia S, et al. Deep learning applied to whole-brain connectome to determine seizure control after epilepsy surgery. Epilepsia 2018;59:1643-1654.

32. de Lanerolle NC, Kim JH, Williamson A, et al. A retrospective analysis of hippocampal pathology in human temporal lobe epilepsy: evidence for distinctive patient subcategories. Epilepsia 2003;44:677-687.

33. Reyes A, Kaestner E, Bahrami N, et al. Cognitive phenotypes in temporal lobe epilepsy are associated with distinct patterns of white matter network abnormalities. Neurology 2019;92:e1957-e1968.

34. Oligschlager S, Huntenburg JM, Golchert J, Lauckner ME, Bonnen T, Margulies DS. Gradients of connectivity distance are anchored in primary cortex. Brain Struct Funct 2017;222:2173-2182.

35. Valk SL, Bernhardt BC, Bockler A, Kanske P, Singer T. Substrates of metacognition on perception and metacognition on higher-order cognition relate to different subsystems of the mentalizing network. Hum Brain Mapp 2016;37:3388-3399.

36. Frauscher B, von Ellenrieder N, Zelmann R, et al. High-Frequency Oscillations in the Normal Human Brain. Ann Neurol 2018;84:374-385.

37. Bartolomei F, Chauvel P, Wendling F. Epileptogenicity of brain structures in human temporal lobe epilepsy: a quantified study from intracerebral EEG. Brain 2008;131:1818-1830.

38. Whelan CD, Altmann A, Botia JA, et al. Structural brain abnormalities in the common epilepsies assessed in a worldwide ENIGMA study. Brain 2018;141:391-408.

39. Misic B, Betzel RF, Nematzadeh A, et al. Cooperative and Competitive Spreading Dynamics on the Human Connectome. Neuron 2015;86:1518-1529.

40. Keller SS, Richardson MP, Schoene-Bake JC, et al. Thalamotemporal alteration and postoperative seizures in temporal lobe epilepsy. Ann Neurol 2015;77:760-774.

41. Tavakol S, Royer J, Lowe AJ, et al. Neuroimaging and connectomics of drug-resistant epilepsy at multiple scales: From focal lesions to macroscale networks. Epilepsia 2019;60:593-604.

42. Lariviere S, Vos de Wael R, Paquola C, et al. Microstructure-Informed Connectomics: Enriching Large-Scale Descriptions of Healthy and Diseased Brains. Brain Connect 2019;9:113-127.

43. van Diessen E, Zweiphenning WJ, Jansen FE, Stam CJ, Braun KP, Otte WM. Brain Network Organization in Focal Epilepsy: A Systematic Review and Meta-Analysis. PLoS One 2014;9:e114606.

44. Otte WM, Dijkhuizen RM, van Meer MP, et al. Characterization of functional and structural integrity in experimental focal epilepsy: reduced network efficiency coincides with white matter changes. PLoS One 2012;7:e39078.

45. Jirsa VK, Stacey WC, Quilichini PP, Ivanov AI, Bernard C. On the nature of seizure dynamics. Brain 2014;137:2210-2230.

46. Schindler KA, Bialonski S, Horstmann MT, Elger CE, Lehnertz K. Evolving functional network properties and synchronizability during human epileptic seizures. Chaos 2008;18:033119.

47. Besson P, Bandt SK, Proix T, et al. Anatomic consistencies across epilepsies: a stereotactic-EEG informed high-resolution structural connectivity study. Brain 2017;140:2639-2652.

48. Khambhati AN, Davis KA, Oommen BS, et al. Dynamic Network Drivers of Seizure Generation, Propagation and Termination in Human Neocortical Epilepsy. PLoS Comput Biol 2015;11:e1004608.

49. Bernhardt BC, Hong SJ, Bernasconi A, Bernasconi N. Magnetic resonance imaging pattern learning in temporal lobe epilepsy: classification and prognostics. Ann Neurol 2015;77:436-446.

50. de Tisi J, Bell GS, Peacock JL, et al. The long-term outcome of adult epilepsy surgery, patterns of seizure remission, and relapse: a cohort study. Lancet 2011;378:1388-1395.

TABLE 1. Patient-specific clinical information.

Patient (side)	**Age** (years)	**Sex**	**Epilepsy duration** (months)	**Post-op. follow-up** (years)	**Surgical outcome**
1 (R)	25	F	7	5	3
2 (R)	17	M	146	7	1
3 (R)	18	M	213	2	2
4 (R)	26	F	194	1	1
5 (R)	26	M	31	2	1
6 (R)	37	F	201	1	3
7 (R)	17	M	67	7	1
8 (R)	29	F	252	1	1
9 (R)	36	M	141	3	1
10 (R)	37	M	248	7	1
11 (R)	22	F	37	6	1
12 (R)	31	F	74	3	1
13 (R)	37	M	333	3	1
14 (R)	15	M	104	3	2
15 (R)	25	F	53	3	1
16 (R)	27	F	72	3	1
17 (R)	16	F	145	2	4
18 (R)	43	M	215	1	1
19 (R)	36	M	2	2	1
20 (L)	25	F	144	1	1
21 (L)	23	F	199	2	3
22 (L)	18	M	190	1	1
23 (L)	17	F	225	2	3
24 (L)	19	F	128	5	1
25 (L)	23	M	84	9	1
26 (L)	37	M	356	1	1
27 (L)	25	M	132	8	2
28 (L)	30	F	77	1	1
29 (L)	22	M	3	2	2
30 (L)	22	M	3	3	4

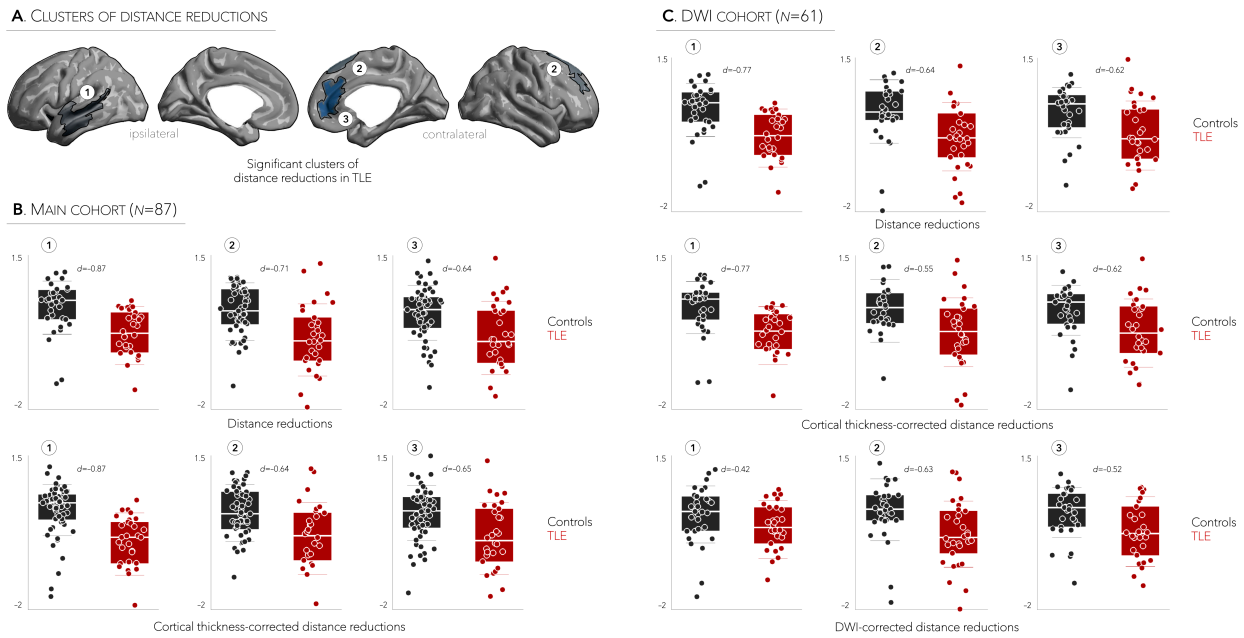

SUPPLEMENTARY FIGURE 1. Effects were robust across main and DWI-only cohorts. a | Clusters of significant distance reductions in TLE patients, relative to controls, are mapped to the surface template. Cohen's *d* values measuring effect sizes for each cluster in **b |** the main cohort and **c |** a subset of participants who underwent additional diffusion MRI.

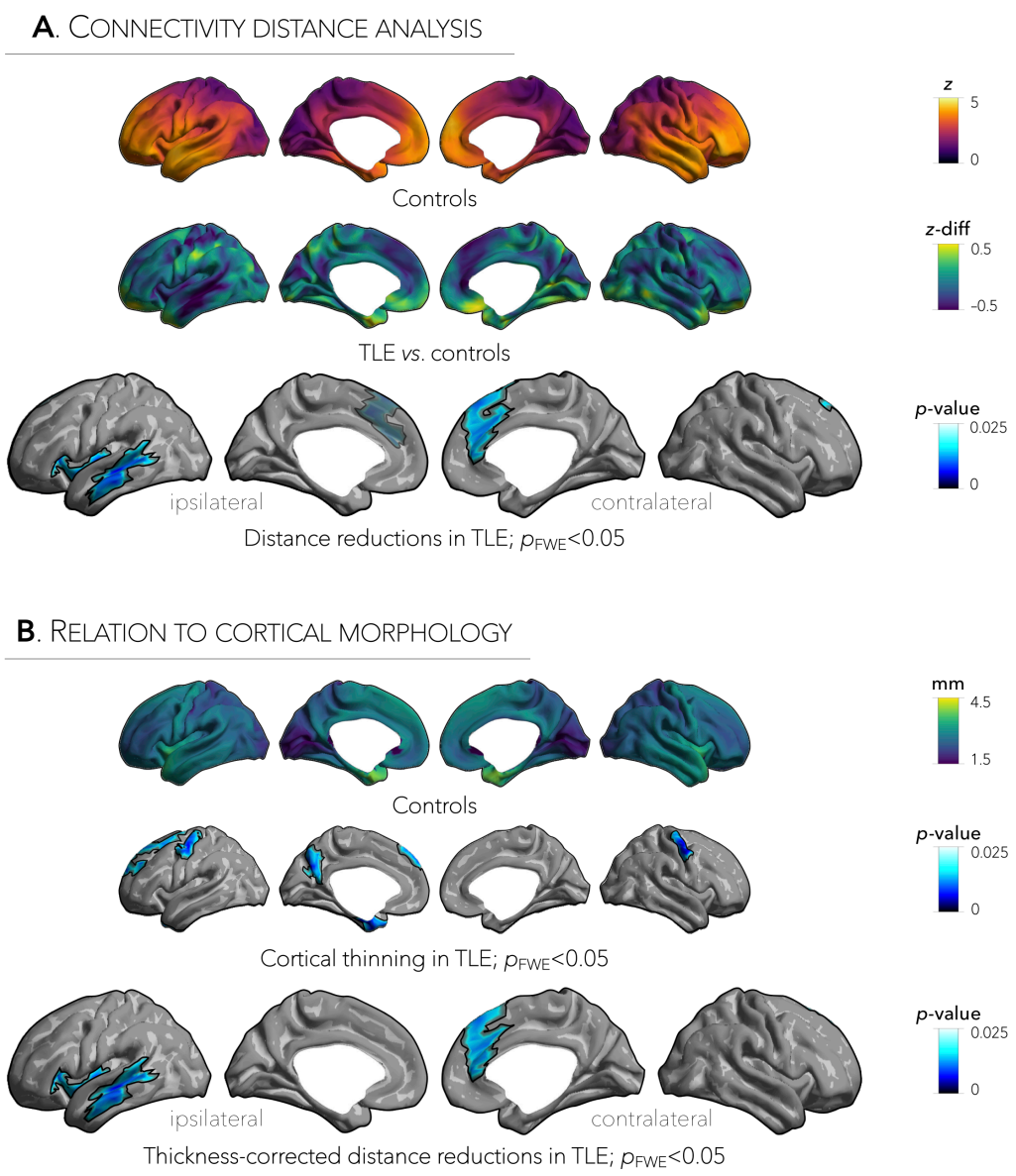

SUPPLEMENTARY FIGURE 2. Connectivity distance findings are replicable in the DWI-only cohort. **a |** Connectivity distance reductions were reproduced in a subset of participants who underwent additional diffusion MRI ($n_{controls}$=31/57, n_{TLE}=30/30) with strongest reduction effects observed in ipsilateral temporo-insular cortices (p<0.01; *FWE*-corrected) and bilateral superior frontal regions (ipsilateral: p=0.06; contralateral: p<0.05; *FWE*-corrected). **b |** Cortical atrophy in patients encompassed bilateral fronto-central and temporal regions (p<0.005; *FWE*-corrected), and was independent of connectivity distance reductions (p<0.01; *FWE*-corrected).